EarlyDetect: Development of tool for early detection of stomach adenocarcinoma based on blood-lipid profile as clinicopathological feature

Om Prakash, Feroz Khan*
Technology Dissemination and Computational Biology Division, CSIR-Central Institute of Medicinal & Aromatic Plants, P.O.-CIMAP, Kukrail Picnic Spot Road, Lucknow-226015 (Uttar Pradesh), India

*Corresponding Author:
Dr. Feroz Khan, Technology Dissemination and Computational Biology Division, CSIR-Central Institute of Medicinal & Aromatic Plants, P.O.-CIMAP, Kukrail Picnic Spot Road, Lucknow-226015 (Uttar Pradesh), INDIA (Email: f.khan@cimap.res.in)

ABSTRACT

Background: Clinicopathological features are used for detection of diseases. Early detection of cancer can be significance for understanding the behavior of disease.

Results: We developed a tool to observe stomach adenocarcinoma in reference of blood-lipid profile. Background of the tool is based on the study made on RNAseq expression analysis of stomach adenocarcinoma. Raw data for study was collected as gene-expression profile from population of cancer-vs-normal. A series of studies performed including: differential gene expression analysis, plasma proteome mapping, extraction of gene-signature enriched with LSTM system model, AI-guided simulation of systems model of gene network, and AI-guided mapping with blood lipid profile to develop R-Shiny web-application.

Conclusion: 'EarlyDetect' is freely available at https://csir-icmr.shinyapps.io/EarlyDetect/. The tool can be utilized for (i) virtual observation of impact of different combinations of lipid profile in cancer progression; (ii) early detection of cancer state for new comer patients.

Keywords: Cancer; Disease; Early; Prediction; Stomach

INTRODUCTION

Blood lipid is a clinicopathological feature which is used to observe disease status. Lipid profile is also useful in detection of cancer as in case of: colorectal, breast, lung, ovarian and prostate cancers etc [1]. Lipid analogs are also known as key regulators of tumorigenesis [2]. Such studies motivate for observation of cancer in relation of lipid profile [3]. Lipid profile shows mutual influence due to drug response. As, hormonal treatment of breast cancer reduces the oestrogen level, which further reduces the blood lipid level [4]. Therefore, blood profile along with percentage of dyslipidemia are observe before chemotherapy [5]. Research is being performed on association between blood lipid level and cancer specific mortalities. Such studies work on variation in blood lipid profile including 'total cholesterol', triglycerides, and HDL/LDL level [6]. Blood lipid level is observed along with blood glucose and extent of inflammation, as in case of ovarian cancer [7]. All these studies suggest that abnormal blood lipid profiles contain association with occurrence of cancer [8]. Therefore, blood lipid profile is

regularly estimated, if cancer patient is under endocrine therapies [9]. Other studies like phospholipid level & peroxidation estimation are performed to understand the malignant neoplasma as in case of breast & uterine cancer [10]. Drug response studies on blood profile are also available for tamoxifen, endoxifen and 4-hydroxyTamoxifen [11]. In totality, potential correlation exists between blood lipid and cancer [12]. Diagnostic values are also considerable in combination of tumor markers and blood lipid [13]. These studies support and prepare a ground for establishing relationship between genotype (tumor markers) and phenotype (blood lipid profile) for observation of import of variation in blood lipid and the cancer status.

RNA expressions are used in several areas of clinical diagnosis [14], including cancer [15]. Categories of RNA as: miRNA [16], circRNA expression [14], long noncoding RNA expression [15], mRNA expression [17] are used in diagnosis. Similar to DNA & protein biomarkers, RNA biomarkers are also potential to discriminate diseased-vs-normal conditions [18]. Therefore, transcriptome sequencing are used in diagnosis of disorders [19]. Transcriptome RNA expressions are used for identification of targetable disease regulatory networks for disease diagnosis [20]. RNA based studies are known with hepatocellular carcinoma [21], colorectal cancer [22], pathway detection [23], prostate tumor [24], and breast cancer [16] etc. RNA expression profile/signature are also used for early diagnosis [25, 26]. Early diagnosis is directly linked with development of biomarker signature (i.e., gene set) with population discrimination capacity [27]. Such studies provide clinically relevant results for diagnosis [28]. These studies provide a ground for accessing RNA expressions as genotypic features for early detection of cancer. Genotype-to-phenotype relation is used also for linking lipid metabolism with cancer related genes [29].

Stomach adenocarcinoma (STAD) is one of the leading reasons of deaths in the world. Lack of early detection is also major barrier behind this situation. Biomarker genes linked with extracellular matrix and platelet-derived growth factor are suggested in early detection of STAD [30]. Besides this, CDCA7-regulated inflammatory mechanism [31], angiogenesis-related lncRNAs [32], PLXNC1 an immune-related gene [33], and Ferroptosis-related gene [34] etc. are also claimed for early detection of STAD. Different stages of STAD are available through prognostic model of TCGA database [35]. Various combination of gene-signature genes is still remained to explore, which creates opportunity to reveal aspect for early detection of STAD.

In present study, blood lipid profile (as phenotype) was linked with gene signature (as genotype) derived for stomach adenocarcinoma, to predict the relative changes/ status of cancer. This process was packaged in the form of R-Shiny GUI web-application named ‘EarlyDetect’.

MATERIALS AND METHOD:

‘EarlyDetect’ establishes relationship between Phenotype and Genotype defined for disease features. It establishes AI-guided relation between blood lipid-profile (clinicopathological phenotype) and expression of gene signature. ‘EarlyDetect’ works as tool for making decision for any unknown sample with blood lipid-profile. Workflow for tool is described as:

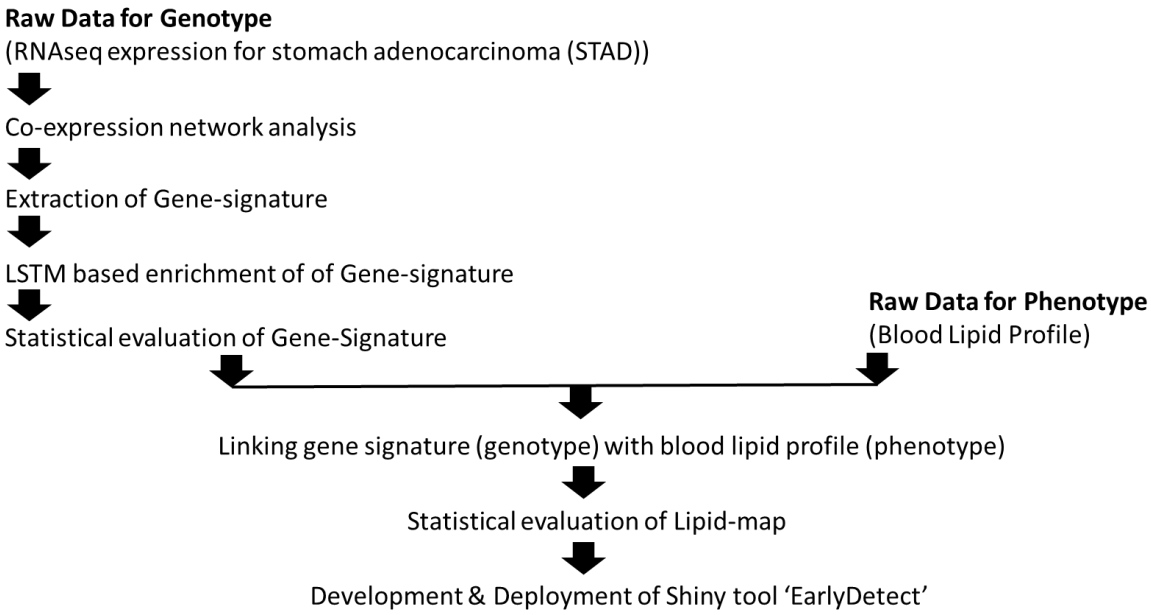

Figure 1. Workflow for Development of tool for early detection of stomach adenocarcinoma based on blood-lipid profile as clinicopathological feature

Phenotype for EarlyDetect:

Although cancer is seeded at molecular level, but it can be featured by clinicopathological phenotypes. Cancer-start-up alters gene expressions. Identification of differentially expressed genes is always a relevant question. Present study deals with establishment of relationship between set of gene expressions (gene signature) and clinicopathological phenotypic character for designing of tool. Prior studies indicate towards the influence of blood lipid-profile (phenotype) during the start-up of cancer. Considering prior studies, blood-lipid profiles featured as phenotype for the study. General blood lipid profile used in this study, is: Total Cholestrol: 200-239(mg/dL); LDL Cholestrol: 130-159 (mg/dL); HDL Cholestrol: 40-60 (mg/dL); Triglycerides: 150-199 (mg/dL); Non-HDL-C: 130-159 (mg/dL); and TG to HDL ratio: 3.0-3.8 (mg/dL).

Genotype for EarlyDetect:

TCGA database provides normalized RNAseq expression for multiple cancer types. TCGA contains 408 independent tumor samples and 211 matching normal tissue samples for Stomach adenocarcinoma (STAD) showing more than 29K genes. Log-fold change in gene expression, above significant threshold, filter outs differentially expressed genes (DEGs). Volcano plot represents DEGs graphically. Since DEGs also display into blood samples; therefore, to filter DEGs, plasma proteome mapped with it. Here mapped DEGs (pDEGs) are DEGs available in blood plasma proteome. Co-expression network analysis processed pDEGs for identification of gene-signature. Details of procedure can be accessed from doi.org/10.1038/s41598-021-87037-w [36]. Gene-wise similarity correlation matrix (scor) & dis-similarity correlation matrix (dcor) presented co-expression of pDEGs. Calculation of scor & dcor takes input of normalized gene expression of pair of genes (G_i & G_j). Here, 'scor' represents the positive correlation

matrix between the genes since the larger value indicates the stronger positive correlation between the pair of genes, while 'dcor' represents the negative correlation between a pair of genes since the larger value indicates the stronger negative correlation between genes, which is also called the distance of a pair of genes. Network analysis used both dissimilarity and similarity matrices with values ranging between 0 & 1. Gene network contained 39 genes. pDEGs in any of these two networks can be considered as co-expressed genes; and therefore, assumed to be involved in existence of system model representing state of disease. Here similarity matrix used for further analysis.

$$scor_{ij} = \frac{1 + \left(\frac{covar(G_i, G_j)}{var(G_i) * var(G_j)}\right)}{2}$$

$$dcor_{ij} = \frac{1 - \left(\frac{covar(G_i, G_j)}{var(G_i) * var(G_j)}\right)}{2}$$

System model, based on pDEGs based on similarity matrix, performed further enrichment of co–expression of gene-set. Long-Short-Term-Memory Recurrent Neural Network (LSTM-RNN) model (implemented in R) simulated the system model. Jacobian matrix performed evaluation of stability of system model. LSTM enriched gene signatures were genotypes. Tool development utilized gene-signature.

Evaluation of signature for capacity of population discrimination: Survival plot, between diseased & normal patients, presents discrimination capacity of gene-signature in the population. Therefore gene-signatures processed for finding survival plot, observed through Logrank p-value < 0.05 as threshold for signaificant expression.

Linking gene signature (genotype) with blood lipid profile (phenotype):
To link genotype with phenotype, LSTM enriched gene signature mapped with lipid-profile of blood. Total 740 (370 (normal) + 370 (cancer)) data-points ranged for gene expression, mapped with lipid-profile. Since, cancer-vs-normal gene expressions are pre-classified, therefore classified gene expression for gene signature made classified mapped lipid-profile dataset. Further, mapped model developed based on the classified genotypic & phenotypic dataset sets, and further utilized for development of map-model for transformation of blood profile into gene expression. Artificial Neural Network (feed-forward backpropagation) mapped the genotype-vs-phenotype profiles. Phenotype contained 06 nodes of blood lipid-profile, while genotype contained 5 nodes of enriched pDEGs.

Evaluation of mapped lipid profile for the capacity of population discrimination: Since genotype used to map phenotype, therefore lipid profile should also contain population discrimination capacity. Therefore, population discrimination capacity was also evaluated for mapped lipid profile. Total 740 (370 (normal) + 370 (cancer)) data-points ranged for lipid-profile mapped in reference of gene-signature.

Two class perceptron classification method utilized mapped lipid-data points for evaluating population discrimination capacity. Area-Under-Curve (AUC) of ROC plot evaluated the classification model.

Deployment of Shiny tool 'EarlyDetect':

R-shiny platform used to develop a web-application, which receive 06 inputs of blood lipid profile, and transform phenotype into gene expression profile with 05 outputs; and further provides output in the form of probability of cancer. The developed application deployed at Shiny-Server.

RESULTS AND DISCUSSION

DEGs for stomach adenocarcinoma in plasma

Total 62 differentially expressed genes found after processing 4644 genes under the thresholds as 'Fold change (log_2)' of 1.5 and 'Significance ($-log_{10}$)' boundary at 0.05 (Figure 2). Furthermore, plasma proteome database (http://www.plasmaproteomedatabase.org) mapping filtered 39 genes out from 62 DEGs (Table 1). These 39 genes (gene symbol marked with 'node ID' from 1 to 39 in table-1) processed strategically for development of gene-signature.

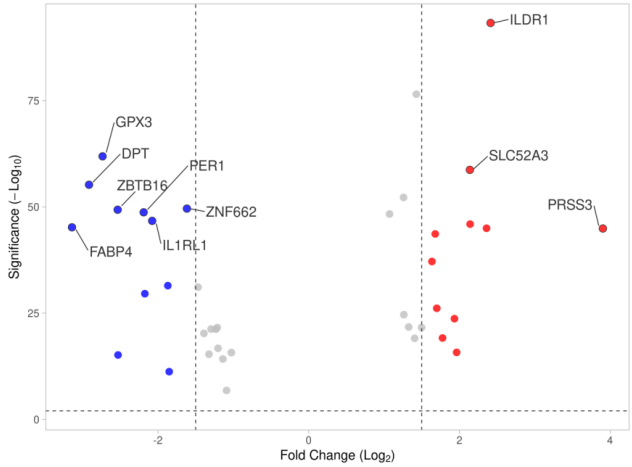

Figure 2. Volcano plot showing differentially expressed genes. Out of 4644 genes, 62 found to be differentially expressed. 'Fold change (log_2)' threshold at 1.5. 'Significance ($-log_{10}$)' boundary was 0.05.

Table 1 Plasma-expressed DEGs. Differentially expressed genes mapped along plasma proteome. 39 genes, out of 62, found to be expressed in blood plasma. Considering the feasibility of patient sampling through blood, plasma proteome expressions used for identification of gene-signature. Here in table each gene symbol is marked with 'node ID' from 1 to 39.

Node ID -vs- Gene	PPD ID	Gene symbol	Gene name	Entrez gene ID
1	HPRD_03272	AFF3	AF4/FMR2 family, member 3	3899
2	HPRD_04087	APBB1	Amyloid beta (A4) precursor protein-binding, family	322

			B, member 1 (Fe65)	
3	HPRD_00134	APOD	Apolipoprotein D	347
4	HPRD_00405	C5	Complement component 5	727
5	HPRD_03148	CHAF1A	Chromatin assembly factor 1, subunit A (p150)	10036
6	HPRD_04592	CHRD	Chordin	8646
7	HPRD_02363	COL4A5	Collagen, type IV, alpha 5	1287
8	HPRD_06012	DPP3	Dipeptidyl-peptidase 3	10072
9	HPRD_00510	DPT	Dermatopontin	1805
10	HPRD_04265	EEF1A2	Eukaryotic translation elongation factor 1 alpha 2	1917
11	HPRD_03225	EFNA3	Ephrin-A3	1944
12	HPRD_03957	PDK4	Pyruvate dehydrogenase kinase, isozyme 4	5166
13	HPRD_06685	PRSS3	Protease, serine, 3	5646
14	HPRD_00340	VCAN	Versican	1462
15	HPRD_03642	NRP1	Neuropilin 1	8829
16	HPRD_06714	SEC23A	Sec23 homolog A (S. Cerevisiae)	10484
17	HPRD_09843	SLC52A3	Solute carrier family 52, riboflavin transporter, member 3	113278
18	HPRD_01418	SERPINE1	Serpin peptidase inhibitor, clade E (nexin, plasminogen activator inhibitor type 1), member 1	5054
19	HPRD_13296	FAM20A	Family with sequence similarity 20, member A	54757
20	HPRD_11762	ZBTB16	Zinc finger and BTB domain containing 16	7704
21	HPRD_01475	PTPN6	Protein tyrosine phosphatase, non-receptor type 6	5777
22	HPRD_01087	LOX	Lysyl oxidase	4015
23	HPRD_03123	IL1RL1	Interleukin 1 receptor-like 1	9173
24	HPRD_09968	G0S2	G0/g1switch 2	50486
25	HPRD_09545	NREP	Neuronal regeneration related protein	9315
26	HPRD_00552	NT5E	5'-nucleotidase, ecto (CD73)	4907
27	HPRD_05081	GPNMB	Glycoprotein (transmembrane) nmb	10457
28	HPRD_01903	ITGAV	Integrin, alpha V	3685
29	HPRD_13735	ILDR1	Immunoglobulin-like domain containing receptor 1	286676
30	HPRD_10420	GFRA3	GDNF family receptor alpha 3	2676
31	HPRD_03115	STC1	Stanniocalcin 1	6781
32	HPRD_04183	IGFBP7	Insulin-like growth factor binding protein 7	3490
33	HPRD_16291	PPP1R14A	Protein phosphatase 1, regulatory (inhibitor) subunit 14A	94274
34	HPRD_02698	FABP4	Fatty acid binding protein 4, adipocyte	2167
35	HPRD_01981	PCCA	Propionyl coa carboxylase, alpha polypeptide	5095
36	HPRD_03774	PER1	Period circadian clock 1	5187
37	HPRD_13516	ZNF662	Zinc finger protein 662	389114
38	HPRD_06631	MAGED4B	Melanoma antigen family D, 4B	81557
39	HPRD_11750	GPX3	Glutathione peroxidase 3 (plasma)	2878

Gene-signature through network analysis

Gene co−expression network analysis performed to know the gene-signature for discrimination of population between disease-vs-normal. Considering 39 gene expression, signatures derived by using above methodology. Notation for Node-vs-Gene should be picked from table above. Two major results found: (A) Out of 39, only 11 genes found to be involved in defining signature through similarity matrix. Similarity network-based signature included AFF3, APBB1, C5, CHRD, COL4A5, EEF1A2, ZBTB16, IL1RL1, GFRA3, ZNF662, and MAGED4B genes; (B) Out of 39, only 10 genes found to be involved in defining signature through dis-similarity matrix. Dis-similarity network-based signature included AFF3, C5, CHAF1A, EFNA3, SLC52A3, LOX, ILDR1, GFRA3, STC1, and ZNF662. Four genes namely AFF3, C5, GFRA3 and ZNF662 were common in both the signatures. Both similarity & dissimilarity network signatures contained population discrimination capacity between normal & diseased (Figure 3). Survival & box plots showed gene-signatures identified (p-value < 0.05) with 11 genes extracted through network analysis (Figure 4). Survival plot validated the capacity of signature for significant discrimination between normal & diseased population.

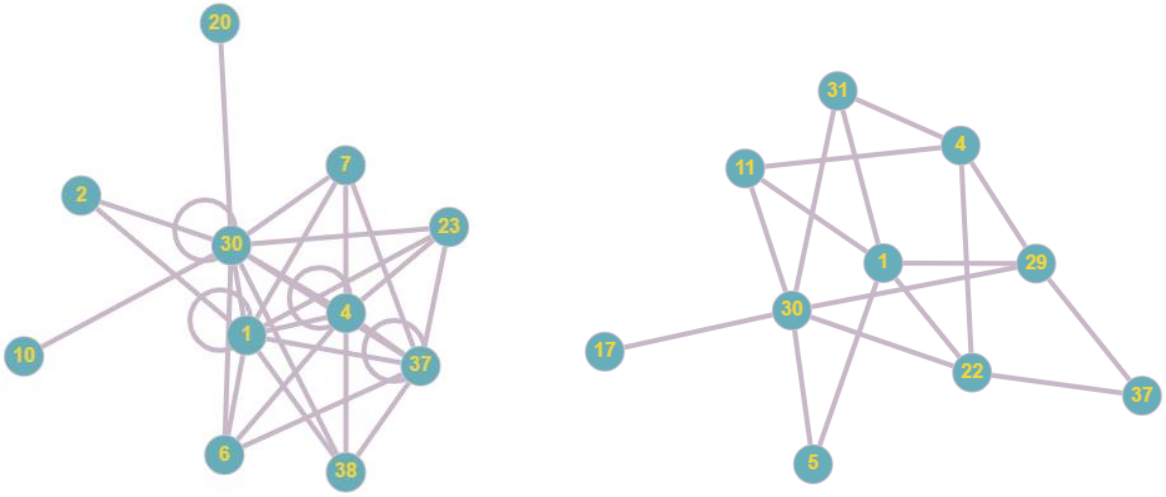

(A) Similarity matrix based signature (B) Dis-similarity matrix based signature

Figure 3. Considering 39 gene expression, signatures derived by the protocol described in above methodology. Signatures were extracted for discrimination between populations of diseased & non-diseased samples. Notation for Node-vs-Gene should be picked from table above. (A) Out of 39, only 11 genes were found to be involved in defining signature through similarity matrix. Similarity network-based signature included AFF3, APBB1, C5, CHRD, COL4A5, EEF1A2, ZBTB16, IL1RL1, GFRA3, ZNF662, and MAGED4B; (B) Out of 39, only 10 genes were found to be involved in defining signature through similarity matrix. Dis-similarity network-based signature included AFF3, C5, CHAF1A, EFNA3, SLC52A3, LOX, ILDR1, GFRA3, STC1, and ZNF662. Both signatures have common involvement of AFF3, C5, GFRA3 and ZNF662.

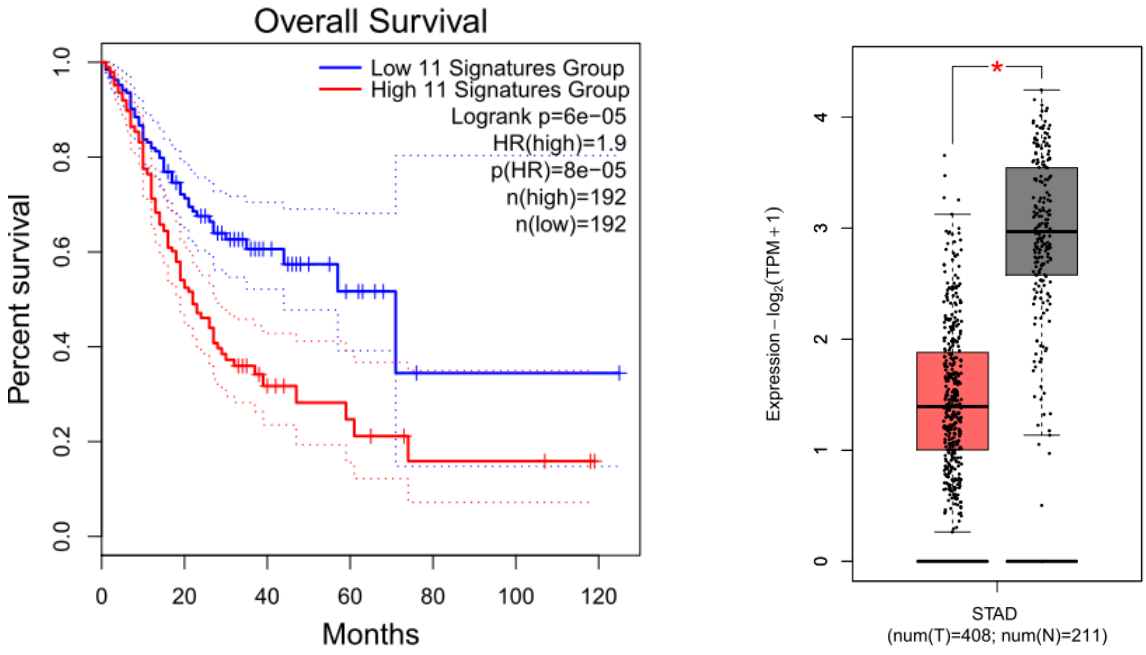

Figure 4. (A) Survival plots in reference of identified gene-signature (p-value < 0.05). Plot derived with 11 genes, extracted through network analysis; (B) Box plots showed the tissue-wise expression of multi-gene signature with 11 gene identified through network analysis.

AI-guided Simulation of systems model & pathway enrichment

Similarity network (including 11 genes) became base for development of AI-guided systems models. Two system models developed; first for normal expression, and second for cancer (tumor) expression. AI-guided simulation of systems model resulted in only 05 genes approaching to stabilized state. Successful simulation involved 05 genes namely AFF3, APBB1, C5, CHRD, and COL4A5. Combination of simulated genes was available in both normal and tumor cases. Expression behavior on time scale also showed different patterns of expression between normal & diseased state (Figure 5(A&B)). Survival & box plots showed in reference of gene-signature identified (p-value < 0.05) with 05 genes extracted through enrichment through system model (Figure 6). It also validated significant discrimination between normal & diseased population. AFF3 gene is known to be a putative transcription activator, that may function in lymphoid development and oncogenesis. APBB1 gene is a Amyloid beta precursor, it role is in response to DNA damage & apoptosis. C5 gene is a Pyrimidine/ purine nucleoside phosphorylase. CHRD gene is a key development protien, and is used during early embryonic tissue and also expression cancer condition. COL4A5 gene is collagen alpha, it is used as constituent of extracellular matrix. Reactome based pathway enrichment analysis showed that, signatures genes belongs to the 'Extracellular Matrix Organization', 'immune system', 'DNA repair' and 'developmental biology'. It is shown that most significant impact on stomach adenocarcinoma is due to genes involved in extracellular matrix organization. In a prior study, STAD early detection biomarker genes were suggested from extracellular matrix [30]. These observations are also in compliance of prior studies on development of gastric cancer [37] (Figure 7). These 05 gene were further used for establishing relation with blood profile.

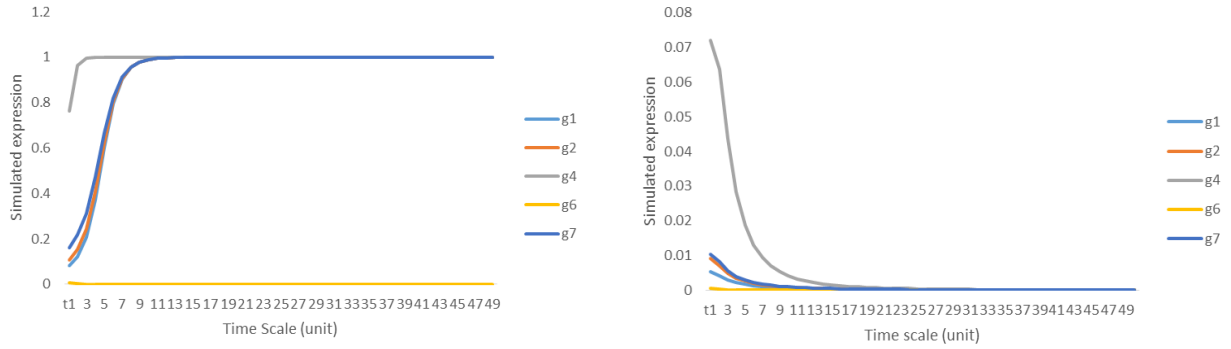

A.(Normal) B.(Tumor)

Figure 5. In present study, above similarity network-based signature (including 11 genes) used for development of AI-guided systems models. Two system models developed; first for normal expression, and second for cancer (tumor) expression. After simulation, it was found that out of 11 gene, only 05 genes (AFF3, APBB1, C5, CHRD, and COL4A5) were involved in successful simulation. Combination of these 05 gene were found in both normal and tumor cases. Above figures A&B showing the patterns of expression 05 gene; discrimination can be easily visualized between normal & tumor case. These expressions have been drawn on the time scale.

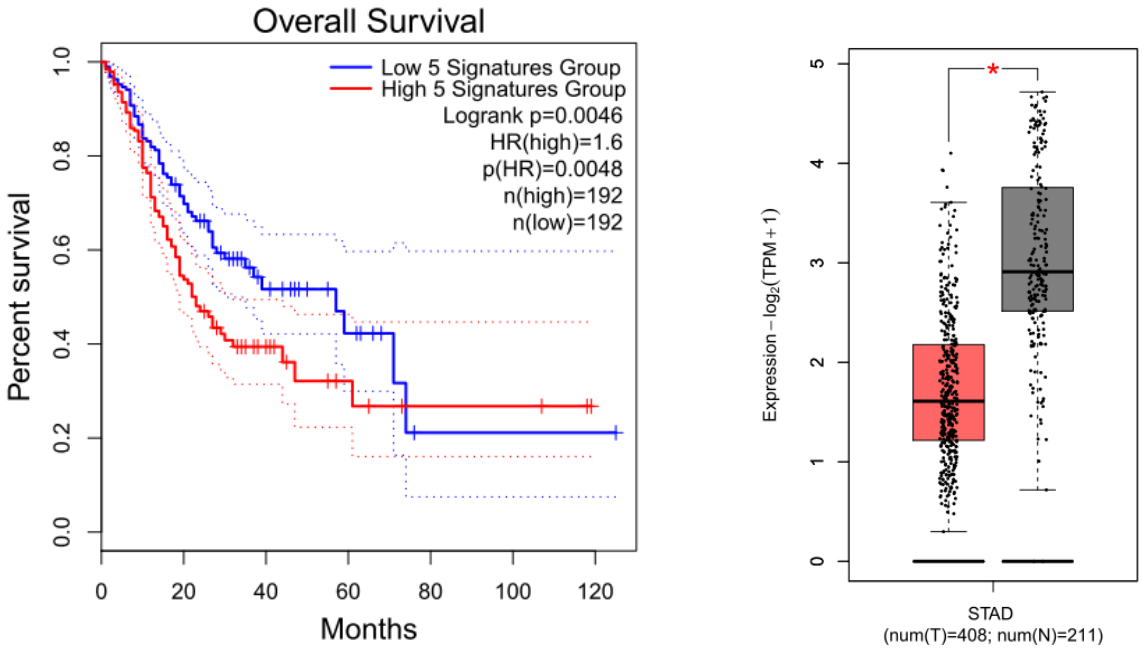

(A) (B)

Figure 6. (A) Survival plot in reference of gene-signature identified (p-value = 0.0046 < 0.05). Plot derived with 05 genes extracted through system model based enrichment of similarity network; (B) Box plot showed the tissue-wise expression of multi-gene signature with 05 gene identified through enrichment of similarity network.

Linking gene signature (genotype) with blood lipid profile (phenotype)

Phenotype blood lipid profile used in this study contain: Total Cholestrol: 200-239(mg/dL); LDL Cholestrol: 130-159 (mg/dL); HDL Cholestrol: 40-60 (mg/dL); Triglycerides: 150-199 (mg/dL); Non-HDL-C: 130-159 (mg/dL); and TG to HDL ratio: 3.0-3.8 (mg/dL). Expression of gene signature further mapped with profile of blood. Normal-to-Cancer discrimination capacity of lipid profile was evaluated through multi-perceptron ANN classification model. Multiple perceptron model architecture of 6-4-2 implemented with learning rate 0.3 and momentum of 0.2 for 500 epochs. Model established with AUC of 0.999 (Table 2, 3, & 4). Furthermore, Genotype-to-Phenotype mapping resulted into ANN model. ANN model implemented in tool developed; where model performs reverse transformation of blood-profile into gene-expression.

Table 2. Confusion matrices showing discrimination capacity of lipid-profile performed by a two-class classification training model and 10-fold cross validation.

Confusion matrix (Training)		
	True	False
Normal	370	0
Tumor	8	362

Confusion matrix (10-fold cross validation)		
	True	False
Normal	369	1
Tumor	3	367

Table 3. Training statistics for two class-classification model for evaluation of discrimination capacity of lipid-profile

	TP	FP	Precision	Recall	F-Measure	MCC	ROC area	PRC area	Class
	1	0.022	0.979	1	0.989	0.979	1	1	T
	0.978	0	1	0.978	0.989	0.979	1	1	N
Weighted Avg.	0.989	0.011	0.989	0.989	0.989	0.979	1	1	

Correctly Classified Instances	732	98.9189 %
Incorrectly Classified Instances	8	1.0811 %
Kappa statistic	0.9784	
Mean absolute error	0.0116	
Root mean squared error	0.0933	
Relative absolute error	2.323 %	
Root relative squared error	18.6595 %	
Total Number of Instances	740	

Table 4. Ten-fold cross-validation statistics for evaluation of two-class classification model showing discrimination capacity of lipid-profile

	TP	FP	Precision	Recall	F-Measure	MCC	ROC area	PRC area	Class
	0.997	0.008	0.992	0.997	0.995	0.989	1	1	T

	0.992	0.003	0.997	0.992	0.995	0.989	1	1	N
Weighted Avg.	0.995	0.005	0.995	0.995	0.995	0.989	1	1	

Correctly Classified Instances	736	99.4595 %
Incorrectly Classified Instances	4	0.5405 %
Kappa statistic	0.9892	
Mean absolute error	0.0091	
Root mean squared error	0.0631	
Relative absolute error	1.8151 %	
Root relative squared error	12.6272 %	
Total Number of Instances	740	

Development of Shiny tool 'EarlyDetect'

The whole study resulted into 'EarlyDetect', which is a R-Shiny web-application. The tool is able to receive any combination of 06 parameters, as inputs of blood lipid profile, and can provide output in the form of probability of status of normal & cancer. It also provides information about the respective variation in gene-expression values in reference of lipid profile. Results can also be seen in tabulated format, including all the parameters & gene expressions. 'EarlyDetect' web application, process blood lipid profile through an ANN model to transform into gene-expression of signature. Further, featured gene expressions is used to calculate classified probability of class weightage of cancer-vs-normal. EarlyDetect predicts probability for both the classes (Figure 7).

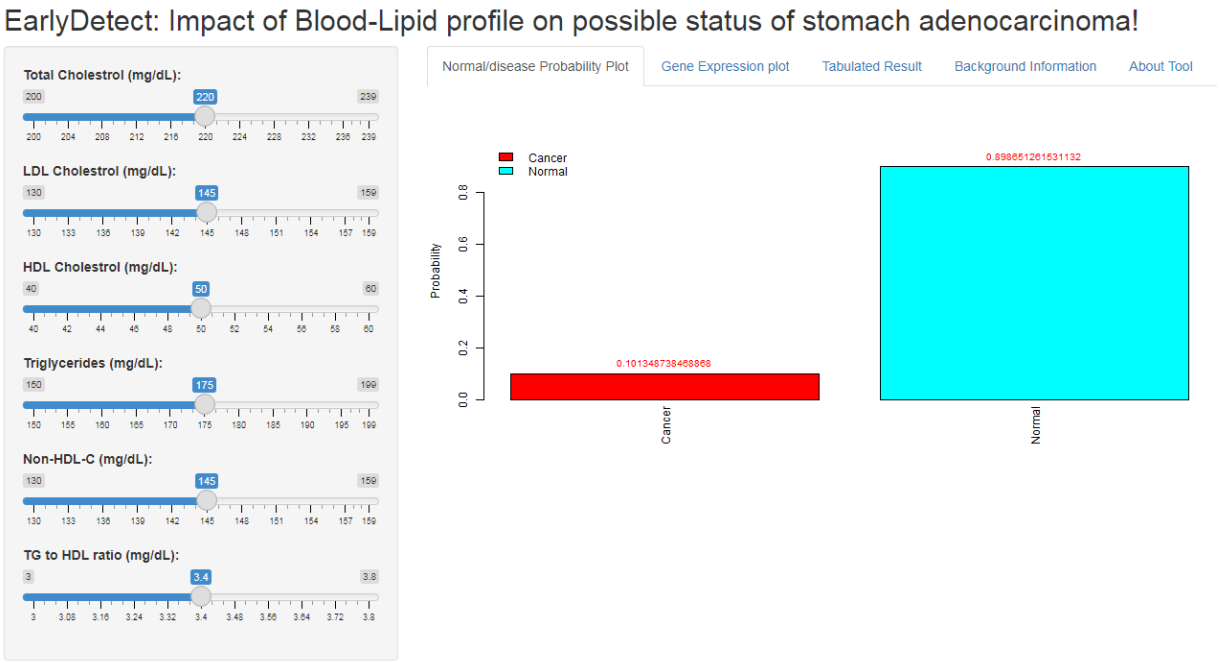

Figure 7. EarlyDetect tool description

Utilization of 'EarlyDetect' for observation of parameter combinations on status of disease

The 'EarlyDetect' proved itself to be highly useful to observe the impact of various combinations of blood lipid profile in probability of cancer. Any combination of lipid profile parameters can be used, from patient, for analysis. Some examples are performed here as: (i) ***which parameter, at its lowest values, has maximum impact on inducing cancer***? To observe this situation, each parameter (one-by-one) was set up at lowest value, taking other parameters to default. It was observed that LDL has maximum impact (about 18%) on creating cancer condition. While probability of cancer further increases with increase in 'TG to HDL ration' parameter up to 20% (Figure 8). (ii) ***What may be the impact of total cholesterol on probability of cancer***? To observe this situation 'total cholesterol value was started from lowest value of 200 mg/dL and increased step by step to maximum value of 239 mg/dL. At each step, probability of cancer was calculated. It was observed that probability of cancer decreases with increases of total cholesterol concentration. This observation was validated through a previous study [38] (Figure 9). It was found that with increase of 'total cholestrol', expression of AFF3, APBB1, C5 and CHRD increased, while expression of COL4A5 get decreased. (iii) ***What is biological relevance of decrease in expression of COL4A5 during increase of total cholestrol***? Decrease in expression of COL4A5 showed reduction in collagen. This observation was validated through a prior study [39] (Figure 10).

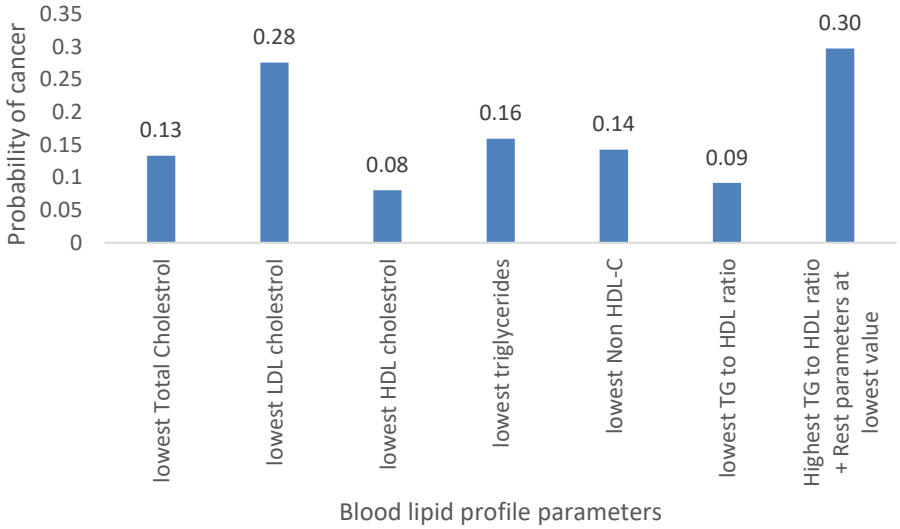

Figure 8. Behavior at the lowest value of each parameter

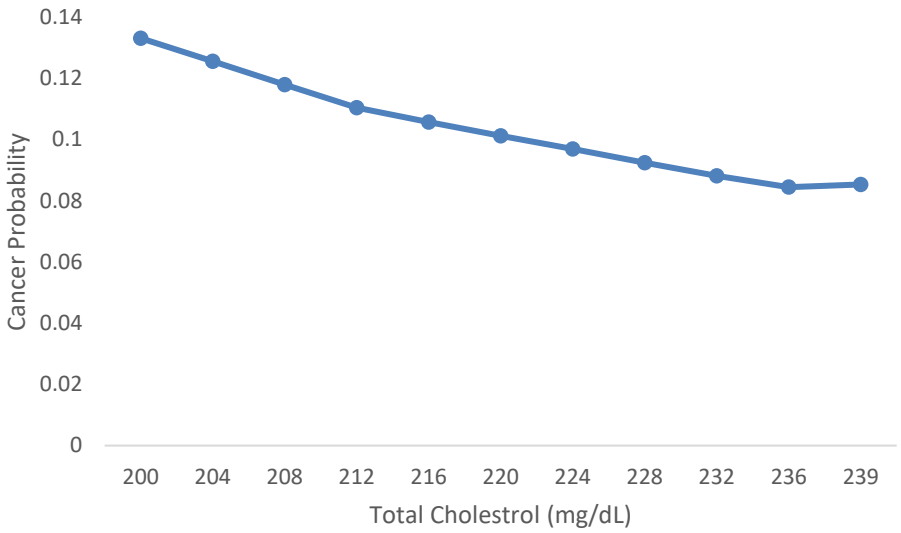

Figure 9. Cancer probability with increase of total cholesterol (mg/dL). Considering result of lipid parameters at their normal state

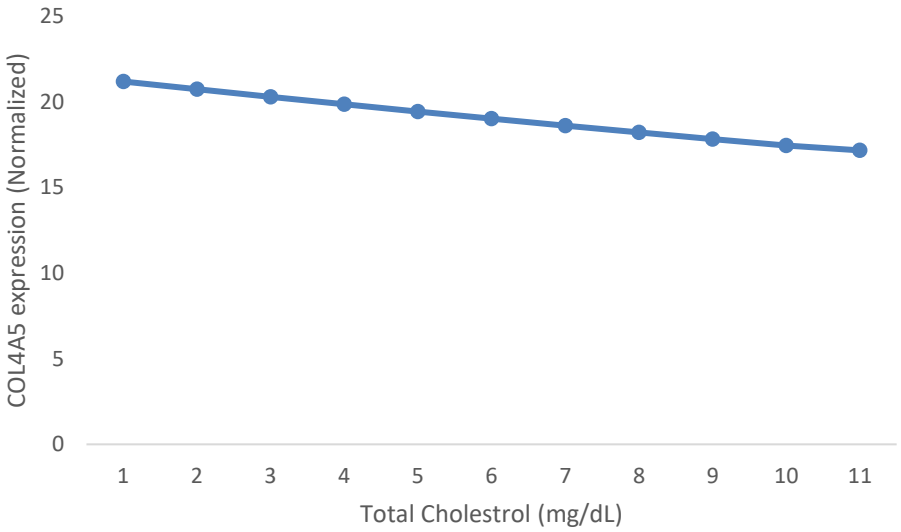

Figure 10. Expression of COL4A5 decreases with increase of total cholesterol (mg/dL). Considering result of lipid parameters at their normal state

Conclusions

Present study successfully established the relationship between phenotype & genotype, as 'blood profile' & 'gene signature' respectively. This relationship was utilized for development of a tool for early detection of stomach adenocarcinoma on the basis of a clinicopathological feature blood-lipid profile. Few identified conclusions based on EarlyDetect tool are as: (i) Low-Density-Lipoprotein cholesterol showed potential impact on creating cancer; (ii) Probability of cancer decreases with increase in total cholesterol; (iii) Collagen decreases with increase in total cholesterol. More conclusions can be drawn through combination studies through 'EarlyDetect'. Tool is freely accessible at 'https://csir-icmr.shinyapps.io/EarlyDetect/'.

Availability and requirements:

Project name: ICMR-RA (IRIS no.: 2020-5987)
Project home page: https://csir-icmr.shinyapps.io/EarlyDetect/
Operating system(s): Platform independent (Online web-Browser).
Programming language: R
Other requirements: Internet access.
License: GNU.
Any restrictions to use by non-academics: No restriction.

Acknowledgement

Authors are thankful to the Director, CSIR-Central Institute of Medicinal & Aromatic Plants (CIMAP), Lucknow, India for infrastructure & research facilities support. Author OP is thankful to the Indian Council of Medical Research (ICMR), New Delhi, India for financial support through RA fellowship (Award letter no. BMI/11(12)/2020, dated: 04/02/2021). Author OP is also thankful to Prof. Thiol Gross, Helmholtz Institute for Functional Marine Biodiversity (HIFMB) at University of OLDENBURG, Germany and Dr. Amit Singh, Chennai Mathematical Institute (CMI) Chennai, India for fruitful suggestions on evaluation of stability of time series systems model. The CSIR-CIMAP publication number of this manuscript is CIMAP/PUB/ 2022/65.

Conflict of interest

There is no conflict of interest.

References

1. Kok DE, van Roermund JG, Aben KK, den Heijer M, Swinkels DW, Kampman E, Kiemeney LA. Blood lipid levels and prostate cancer risk; a cohort study. Prostate Cancer Prostatic Dis. 2011 Dec;14(4):340-5. doi: 10.1038/pcan.2011.30. Epub 2011 Jul 5. PMID: 21727905.
2. Dong Y, Wang H, Shan D, Yu Z. [Research Progress on the Relationship between Blood Lipids and ?Lung Cancer Risk and Prognosis]. Zhongguo Fei Ai Za Zhi. 2020 Sep 20;23(9):824-829. Chinese.

doi: 10.3779/j.issn.1009-3419.2020.102.36. Epub 2020 Aug 10. PMID: 32773011; PMCID: PMC7519960.

3. Xiong Z, Lin Y, Yu Y, Zhou X, Fan J, Rog CJ, Cai K, Wang Z, Chang Z, Wang G, Tao K, Cai M. Exploration of Lipid Metabolism in Gastric Cancer: A Novel Prognostic Genes Expression Profile. Front Oncol. 2021 Sep 8;11:712746. doi: 10.3389/fonc.2021.712746. PMID: 34568042; PMCID: PMC8457048.
4. Bundred NJ. The effects of aromatase inhibitors on lipids and thrombosis. Br J Cancer. 2005 Aug;93 Suppl 1(Suppl 1):S23-7. doi: 10.1038/sj.bjc.6602692. PMID: 16100522; PMCID: PMC2361692.
5. Xu L, Dong Q, Long Y, Tang X, Zhang N, Lu K. Dynamic Changes of Blood Lipids in Breast Cancer Patients After (Neo)adjuvant Chemotherapy: A Retrospective Observational Study. Int J Gen Med. 2020 Oct 14;13:817-823. doi: 10.2147/IJGM.S273056. PMID: 33116773; PMCID: PMC7569068.
6. Yang Y, Gao G, Shi J, Zhang J. Increased Blood Lipid Level is Associated with Cancer-Specific Mortality and All-Cause Mortality in Patients with Colorectal Cancer (=65 Years): A Population-Based Prospective Cohort Study. Risk Manag Healthc Policy. 2020 Jul 23;13:855-863. doi: 10.2147/RMHP.S260113. Retraction in: Risk Manag Healthc Policy. 2021 Jul 21;14:3057. PMID: 32801961; PMCID: PMC7399450.
7. Li G, Zhang K, Gong F, Jin H. A study on changes and clinical significance of blood glucose, blood lipid and inflammation in patients with ovarian cancer. J BUON. 2019 Nov-Dec;24(6):2322-2326. PMID: 31983101.
8. Halton JM, Nazir DJ, McQueen MJ, Barr RD. Blood lipid profiles in children with acute lymphoblastic leukemia. Cancer. 1998 Jul 15;83(2):379-84. PMID: 9669823.
9. Engan T. Magnetic resonance spectroscopy of blood plasma lipoproteins in malignant disease: methodological aspects and clinical relevance. Anticancer Res. 1996 May-Jun;16(3B):1461-71. PMID: 8694514.
10. Kotrikadze NG, Tsartsidze MA, Dzhishkariani OS, Londaridze AM, Lomsadze BA. Izuchenie fosfolipidnogo sostava lipidov krovi pri rake molochnoi zhelezy i tela matki [Phospholipid composition of blood lipids in breast and uterine cancer]. Eksp Onkol. 1987;9(2):68-70. Russian. PMID: 3582245.
11. Siqueira MLS, Andrade SMV, Vieira JLF, Monteiro MC. A preliminary study on the association of tamoxifen, endoxifen, and 4-hydroxytamoxifen with blood lipids in patients with breast cancer. Biomed Pharmacother. 2021 Oct;142:111972. doi: 10.1016/j.biopha.2021.111972. Epub 2021 Aug 11. PMID: 34391185.
12. Jin W, Shan B, Liu H, Li W, Zhang Q, Zhou S, Hu D, Pan Y. The correlation between blood lipids and clinicopathological features of breast cancer in young females. Gland Surg. 2020 Oct;9(5):1443-1449. doi: 10.21037/gs-20-616. PMID: 33224819; PMCID: PMC7667059.
13. Jiang M, Ding G, Li G. Diagnostic value of combined detection of multiple tumor markers and blood lipid indexes in colorectal cancer and its prediction on adverse reactions of chemotherapy. J BUON. 2021 Jul-Aug;26(4):1226-1230. PMID: 34564974.
14. Dube U, Del-Aguila JL, Li Z, Budde JP, Jiang S, Hsu S, Ibanez L, Fernandez MV, Farias F, Norton J, Gentsch J, Wang F; Dominantly Inherited Alzheimer Network (DIAN), Salloway S, Masters CL, Lee

JH, Graff-Radford NR, Chhatwal JP, Bateman RJ, Morris JC, Karch CM, Harari O, Cruchaga C. An atlas of cortical circular RNA expression in Alzheimer disease brains demonstrates clinical and pathological associations. Nat Neurosci. 2019 Nov;22(11):1903-1912. doi: 10.1038/s41593-019-0501-5. Epub 2019 Oct 7. PMID: 31591557; PMCID: PMC6858549.

15. Lorenzi L, Avila Cobos F, Decock A, Everaert C, Helsmoortel H, Lefever S, Verboom K, Volders PJ, Speleman F, Vandesompele J, Mestdagh P. Long noncoding RNA expression profiling in cancer: Challenges and opportunities. Genes Chromosomes Cancer. 2019 Apr;58(4):191-199. doi: 10.1002/gcc.22709. Epub 2019 Jan 20. PMID: 30461116.
16. Liu D, Li B, Shi X, Zhang J, Chen AM, Xu J, Wang W, Huang K, Gao J, Zheng Z, Liu D, Wang H, Shi W, Chen L, Xu J. Cross-platform genomic identification and clinical validation of breast cancer diagnostic biomarkers. Aging (Albany NY). 2021 Jan 20;13(3):4258-4273. doi: 10.18632/aging.202388. Epub 2021 Jan 20. PMID: 33493140; PMCID: PMC7906147.
17. Ruan GT, Zhu LC, Gong YZ, Liao XW, Wang XK, Liao C, Wang S, Yan L, Xie HL, Zhou X, Li YZ, Gao F. The diagnosis and prognosis values of WNT mRNA expression in colon adenocarcinoma. J Cell Biochem. 2020 Jun;121(5-6):3145-3161. doi: 10.1002/jcb.29582. Epub 2019 Dec 30. PMID: 31886580.
18. Wang L, Zeng L, Jiang H, Li Z, Liu R. Microarray Profile of Long Noncoding RNA and Messenger RNA Expression in a Model of Alzheimer's Disease. Life (Basel). 2020 May 14;10(5):64. doi: 10.3390/life10050064. PMID: 32423012; PMCID: PMC7281340.
19. Akula N, Marenco S, Johnson K, Feng N, Zhu K, Schulmann A, Corona W, Jiang X, Cross J, England B, Nathan A, Detera-Wadleigh S, Xu Q, Auluck PK, An K, Kramer R, Apud J, Harris BT, Harker Rhodes C, Lipska BK, McMahon FJ. Deep transcriptome sequencing of subgenual anterior cingulate cortex reveals cross-diagnostic and diagnosis-specific RNA expression changes in major psychiatric disorders. Neuropsychopharmacology. 2021 Jun;46(7):1364-1372. doi: 10.1038/s41386-020-00949-5. Epub 2021 Feb 8. PMID: 33558674; PMCID: PMC8134494.
20. Gaffo E, Buratin A, Dal Molin A, Bortoluzzi S. Bioinformatic Analysis of Circular RNA Expression. Methods Mol Biol. 2021;2348:343-370. doi: 10.1007/978-1-0716-1581-2_22. PMID: 34160817.
21. Chen D, Zhang C, Lin J, Song X, Wang H. Screening differential circular RNA expression profiles reveal that hsa_circ_0128298 is a biomarker in the diagnosis and prognosis of hepatocellular carcinoma. Cancer Manag Res. 2018 May 18;10:1275-1283. doi: 10.2147/CMAR.S166740. PMID: 29849467; PMCID: PMC5965387.
22. Mamelli RE, Felipe AV, Silva TD, Hinz V, Forones NM. RNAM EXPRESSION AND DNA METHYLATION OF DKK2 GENE IN COLORECTAL CÂNCER. Arq Gastroenterol. 2021 Jan-Mar;58(1):55-60. doi: 10.1590/S0004-2803.202100000-10. PMID: 33909798.
23. Wu J, Fang X, Huang H, Huang W, Wang L, Xia X. Construction and topological analysis of an endometriosis-related exosomal circRNA-miRNA-mRNA regulatory network. Aging (Albany NY). 2021 Apr 26;13(9):12607-12630. doi: 10.18632/aging.202937. Epub 2021 Apr 26. PMID: 33901012; PMCID: PMC8148458.
24. Xia Q, Ding T, Zhang G, Li Z, Zeng L, Zhu Y, Guo J, Hou J, Zhu T, Zheng J, Wang J. Circular RNA Expression Profiling Identifies Prostate Cancer- Specific circRNAs in Prostate Cancer. Cell Physiol Biochem. 2018;50(5):1903-1915. doi: 10.1159/000494870. Epub 2018 Nov 5. PMID: 30396163.

25. Zheng S, Li J, Hou L, Li J. Identifying RNA Biomarkers for Oesophageal Squamous Cell Carcinoma. Stud Health Technol Inform. 2019 Aug 21;264:1084-1088. doi: 10.3233/SHTI190392. PMID: 31438092.
26. Liu Z, Meng H, Fang M, Guo W. Identification and Potential Mechanisms of a 7-MicroRNA Signature That Predicts Prognosis in Patients with Lower-Grade Glioma. J Healthc Eng. 2021 Nov 20;2021:3251891. doi: 10.1155/2021/3251891. PMID: 34845420; PMCID: PMC8627350.
27. Yang H, Su H, Hu N, Wang C, Wang L, Giffen C, Goldstein AM, Lee MP, Taylor PR. Integrated analysis of genome-wide miRNAs and targeted gene expression in esophageal squamous cell carcinoma (ESCC) and relation to prognosis. BMC Cancer. 2020 May 6;20(1):388. doi: 10.1186/s12885-020-06901-6. PMID: 32375686; PMCID: PMC7201714.
28. Brakenridge SC, Starostik P, Ghita G, Midic U, Darden D, Fenner B, Wacker J, Efron PA, Liesenfeld O, Sweeney TE, Moldawer LL. A Transcriptomic Severity Metric That Predicts Clinical Outcomes in Critically Ill Surgical Sepsis Patients. Crit Care Explor. 2021 Oct 14;3(10):e0554. doi: 10.1097/CCE.0000000000000554. PMID: 34671746; PMCID: PMC8522866.
29. Kale A, Aldahish A, Shah G. Calcitonin receptor is required for T-antigen-induced prostate carcinogenesis. Oncotarget. 2020 Mar 3;11(9):858-874. doi: 10.18632/oncotarget.27495. PMID: 32180899; PMCID: PMC7061735.
30. Tan R, Zhang G, Liu R, Hou J, Dong Z, Deng C, Wan S, Lai X, Cui H. Identification of Early Diagnostic and Prognostic Biomarkers via WGCNA in Stomach Adenocarcinoma. Front Oncol. 2021 Jun 18;11:636461. doi: 10.3389/fonc.2021.636461. PMID: 34221961; PMCID: PMC8249817.
31. Guo Y, Zhou K, Zhuang X, Li J, Shen X. CDCA7-regulated inflammatory mechanism through TLR4/NF-?B signaling pathway in stomach adenocarcinoma. Biofactors. 2021 Sep;47(5):865-878. doi: 10.1002/biof.1773. Epub 2021 Aug 2. PMID: 34339079.
32. Han C, Zhang C, Wang H, Li K, Zhao L. Angiogenesis-related lncRNAs predict the prognosis signature of stomach adenocarcinoma. BMC Cancer. 2021 Dec 7;21(1):1312. doi: 10.1186/s12885-021-08987-y. PMID: 34876056; PMCID: PMC8653638.
33. Ni Z, Huang C, Zhao H, Zhou J, Hu M, Chen Q, Ge B, Huang Q. PLXNC1: A Novel Potential Immune-Related Target for Stomach Adenocarcinoma. Front Cell Dev Biol. 2021 Jul 2;9:662707. doi: 10.3389/fcell.2021.662707. PMID: 34277610; PMCID: PMC8283001.
34. Xiao R, Wang S, Guo J, Liu S, Ding A, Wang G, Li W, Zhang Y, Bian X, Zhao S, Qiu W. Ferroptosis-related gene NOX4, CHAC1 and HIF1A are valid biomarkers for stomach adenocarcinoma. J Cell Mol Med. 2022 Feb;26(4):1183-1193. doi: 10.1111/jcmm.17171. Epub 2022 Jan 13. PMID: 35023280; PMCID: PMC8831942.
35. Qian H, Cui N, Zhou Q, Zhang S. Identification of miRNA biomarkers for stomach adenocarcinoma. BMC Bioinformatics. 2022 May 16;23(1):181. doi: 10.1186/s12859-022-04719-6. PMID: 35578189; PMCID: PMC9112558.
36. Vizeacoumar FS, Guo H, Dwernychuk L, Zaidi A, Freywald A, Wu FX, Vizeacoumar FJ, Ahmed S. Mining the plasma-proteome associated genes in patients with gastro-esophageal cancers for biomarker discovery. Sci Rep. 2021 Apr 7;11(1):7590. doi: 10.1038/s41598-021-87037-w. PMID: 33828156; PMCID: PMC8027878.

37. Moreira AM, Pereira J, Melo S, Fernandes MS, Carneiro P, Seruca R, Figueiredo J. The Extracellular Matrix: An Accomplice in Gastric Cancer Development and Progression. Cells. 2020 Feb 8;9(2):394. doi: 10.3390/cells9020394. PMID: 32046329; PMCID: PMC7072625.
38. Mayengbam SS, Singh A, Pillai AD, Bhat MK. Influence of cholesterol on cancer progression and therapy. Transl Oncol. 2021 Jun;14(6):101043. doi: 10.1016/j.tranon.2021.101043. Epub 2021 Mar 20. PMID: 33751965; PMCID: PMC8010885.
39. Plenz G, Dorszewski A, Völker W, Ko YS, Severs NJ, Breithardt G, Robenek H. Cholesterol-induced changes of type VIII collagen expression and distribution in carotid arteries of rabbit. Arterioscler Thromb Vasc Biol. 1999 Oct;19(10):2395-404. doi: 10.1161/01.atv.19.10.2395. PMID: 10521369.